ACS APPLIED MATERIALS & INTERFACES

Letter

www.acsami.org

New Potassium–Sodium Niobate Ceramics with a Giant d_{33}

Xiaopeng Wang,[†] Jiagang Wu,*[,†] Dingquan Xiao,[†] Xiaojing Cheng,[†] Ting Zheng,[†] Xiaojie Lou,[‡] Binyu Zhang,[†] and Jianguo Zhu[†]

[†]Department of Materials Science, Sichuan University, Chengdu 610064, P. R. China

[‡]Multi-disciplinary Materials Research Center, Frontier Institute of Science and Technology, Xi'an Jiaotong University, Xi'an 710054, P. R. China

Supporting Information

ABSTRACT: For potassium–sodium niobate, poor piezoelectric properties always perplex most researchers, and then it becomes important to attain a giant piezoelectricity. Here we reported a giant piezoelectric constant in $(1-x)(K_{0.48}Na_{0.52})(Nb_{0.95}Sb_{0.05})O_3$-$xBi_{0.5}Ag_{0.5}ZrO_3$ lead-free ceramics. The rhombohedral-tetragonal phase boundary was shown in the ceramics with $0.04 < x \leq 0.05$, and then the ceramic with $x = 0.0425$ possesses a giant d_{33} of ~490 pC/N. We also discussed the physical mechanisms of enhanced piezoelectricity. As a result, such a research can benefit the sustainable development of $(K,Na)NbO_3$ materials.

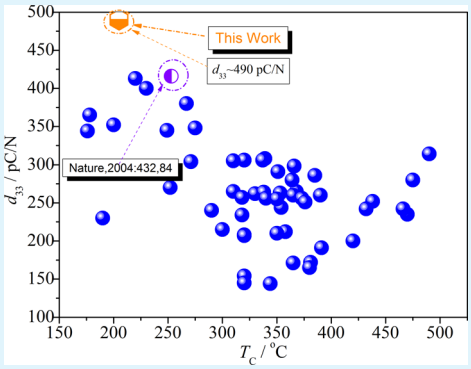

KEYWORDS: *lead-free ceramics, potassium–sodium niobate, high piezoeletricicty*

In the past decades, the objective of most researchers is to develop one kind of $(K,Na)NbO_3$ (KNN) lead-free ceramics with a high piezoelectric constant (d_{33}),[1−24] which is superior or comparable to those of KNN-textured ones[1] and part Pb(Zr, Ti)O_3 (PZT) ones.[25,26] Some useful methods were dedicated to enhance the piezoelectricicty of KNN ceramics, such as the reactive-templated grain growth,[1] the construction of phase boundary,[1,3,4,6−13,15−22] the sintering aids,[14,23] and new preparation technique.[24] In contrast, all reported results of KNN-based materials depressed most researchers,[2−24] and their d_{33}[2−24] is still inferior to that (~416 pC/N) of the textured KNN-based ceramics with Li^+, Ta^{5+}, and Sb^{5+}.[1] Therefore, those research results may make us believe that the d_{33} of ~416 pC/N is an insurmountable bottleneck for KNN-based ceramics.

We stick to believing that the construction of phase boundary is a necessary tool to promote the d_{33} of KNN-based ceramics according to recent research development.[9,16,21,22] In the past ten years, three kinds of phase boundaries have been considered and applied for KNN-based ceramics, including rhombohedral orthorhombic (R-O),[27,28] orthorhombic-tetragonal (O-T),[1,3,4,8−10,17,19] and rhombohedral-tetragonal (R-T) phase boundaries.[16,20−22] Among three phase boundaries, the O-T phase boundary becomes most popular in the whole research development of KNN-based materials[1,3,4,8−10,17,19] because a big breakthrough of d_{33} firstly results from the formation of such a phase boundary.[1] However, a rather poor piezoelectricity of KNN-based ceramics is always induced by forming the R-O phase boundary.[27,28] In the past seven years, we have conducted lots of related KNN experiments to understand the bottleneck of hindering the improvement in d_{33}, and found that the R-T phase boundary could solve such an issue.[16,22,29]

Here we designed a new material system of $(1-x)$-$(K_{0.48}Na_{0.52})(Nb_{0.95}Sb_{0.05})O_3$ -$xBi_{0.5}Ag_{0.5}ZrO_3$ [$(1-x)$KNNS-xBAZ], and the R-T phase boundary was mediated by tailoring BAZ contents. In this work, doping both Sb^{5+}[27] and BAZ can tune their T_{R-O} and T_{O-T}, finally inducing the formation of R-T phase boundary. A giant d_{33} of ~490 pC/N were obtained in the ceramic with $x = 0.0425$ because of the involved R-T phase boundary. Such a d_{33} of this work is superior to other reported results of KNN-based ceramics.[2−24] Moreover, the underlying physical mechanisms for the involved R-T phase boundary and the enhanced piezoelectricity were also emphasized.

In the present work, the phase structure of the ceramics is analyzed by considering XRD patterns and ε_r-T curves, as shown in Figure 1−3. Figure 1a gives the XRD patterns of the ceramics in $2\theta = 20-60°$. All the ceramics show a pure phase. Figure 1b displays the expanded XRD patterns of the ceramics in $2\theta = 43-47°$. The different peak shapes are involved as the BAZ changes. For further detecting their phase evolution, we measured their ε_r-T curves in -150−180 °C, as shown in Figure 2a−g. By considering both XRD data and ε_r vs. T curves, we can understand the change of their phase structures, as shown below: These ceramics with $x \leq 0.02$ are an O phase, as

Received: February 8, 2014
Accepted: April 25, 2014
Published: May 1, 2014

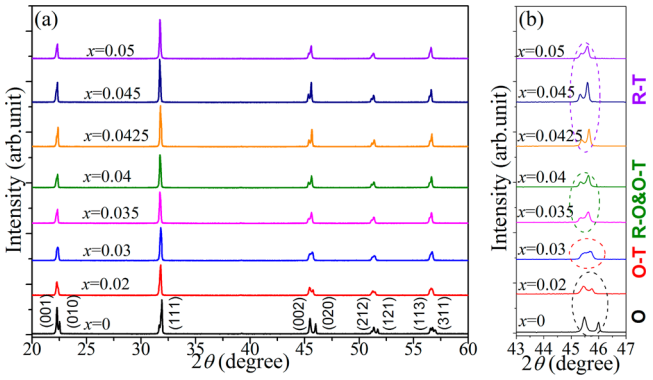

Figure 1. XRD patterns of the ceramics measured at (a) 2θ = 20−60° and (b) 2θ = 43−47°.

confirmed by the XRD patterns as well as $T_{R\text{-}O} \approx -41$ °C and $T_{O\text{-}T} \approx 107$ °C for x = 0.02. As the x increases, the O and T phase coexistence is demonstrated in x = 0.03, and $T_{R\text{-}O}$ and $T_{O\text{-}T}$ gradually move together (see Figure 2b). As the x further rises, $T_{R\text{-}O}$ and $T_{O\text{-}T}$ of the ceramics with 0.03 < $x \leq$ 0.04 were observed near room temperature, as shown in Figures 1 and 2c, d. Finally, the $T_{R\text{-}T}$ was formed in the ceramics with 0.04 < $x \leq$ 0.05, as shown in Figures 1 and 2e−g. Therefore, the phase structure is identified in those ceramics, as listed below: O for 0 $\leq x \leq$ 0.02, O-T for 0.02 < $x \leq$ 0.03, R-O&O-T for 0.03 < $x \leq$ 0.04, and R-T for 0.04 < $x \leq$ 0.05.

Figure 3a plots the ε_r vs. T curves of the ceramics with 0 $\leq x \leq$ 0.05, conducted in 30−450 °C and $f \approx$ 100 kHz. The ceramics with $x \leq$ 0.03 have two dielectric peaks for ε_r vs. T, which are assigned to $T_{O\text{-}T}$ and T_C. However, only one dielectric peak for ε_r vs. T is shown in 0.03 < $x \leq$ 0.05. Figure 3b displays the phase diagram of the ceramics according to the ε_r vs. T curves of Figures 2 and 3a. As the BAZ rises from 0 to 0.05, T_C and $T_{O\text{-}T}$ drop, and $T_{R\text{-}O}$ increases. With increasing BAZ content, $T_{R\text{-}O}$ and $T_{O\text{-}T}$ of the ceramics with 0.04 < $x \leq$ 0.05 move together, confirming the formation of R-T phase boundary. Here the objective of doping Zr^{4+} is to mainly increase $T_{R\text{-}O}$, adding $[Bi_{0.5}Ag_{0.5}]^{2+}$ decreases $T_{O\text{-}T}$. As a result, the ceramics with 0.04 < $x \leq$ 0.05 have a coexistence of R and T phases.

Figure 4a plots composition dependence of both ε_r and tan δ of the ceramics, measured at 100 kHz and 25 °C. The ε_r first increases and subsequently drops, reaching a maximum value for R-T phase boundary. In addition, the peak ε_r further confirms the involved R-T phase boundary of the ceramics with 0.04 < $x \leq$ 0.05.[7] These ceramics with 0.03 $\leq x \leq$ 0.05 have a lower tan δ than those of the ones with $x \leq$ 0.02 because of the dense microstructure (see Figure S1 in the Supporting Information). As a result, the ceramic with x = 0.0425 has enhanced dielectric properties (e.g., $\varepsilon_r \sim$ 2830 and tan $\delta \sim$ 3.5%). Figure 4b displays the composition dependence of P−E loops of the ceramics, carried out at f = 10 Hz and 25 °C. A P−E loop was found in all the samples, and their shape depends on the BAZ contents. Figure 4c plots the composition dependence of P_r and E_C in order to understand the influence of BAZ content on ferroelectric properties, where the P_r and E_C derived from Figure 4b. The P_r first rises, reaches the maximum 12.1−15.5 μC/cm^2 for x = 0.02−0.045, and then drops with increasing BAZ content. However, their E_C presents different trend, that is, it almost decreases from 12.7 kV/cm to 7.8 kV/cm as the BAZ rises. Figure 4d plots the composition dependence of their d_{33} and k_p The d_{33} dramatically rises and drops with increasing BAZ content, giving a maximum value of ~490 pC/N at x = 0.0425. The ceramics located at R-T phase boundary zone also show an enhanced k_p. Therefore, enhanced dielectric and piezoelectric properties (e.g., $\varepsilon_r \approx$ 2830, tan $\delta \approx$ 3.5%, $d_{33} \approx$ 490 pC/N, and $k_p \approx$ 46.0%) were shown in the ceramic with x = 0.0425. In this work, the d_{33} is much larger than other reported results of KNN-based ceramics,[2−24,27,28] including the KNN-textured ceramics,[1] and is also larger than those of part PZT ceramics.[25,26]

Subsequently, the origin of a giant d_{33} in this material was analyzed. First, the R-T phase boundary could be largely attributed to the origin of giant d_{33} of this work.[8,9,12] It is well known that the origin of ultra-high piezoelectricity in lead-based materials is due to coexistence of the R and T phases, where a highly domain orientation results from the existence of two thermodynamically equivalent phases during the poling

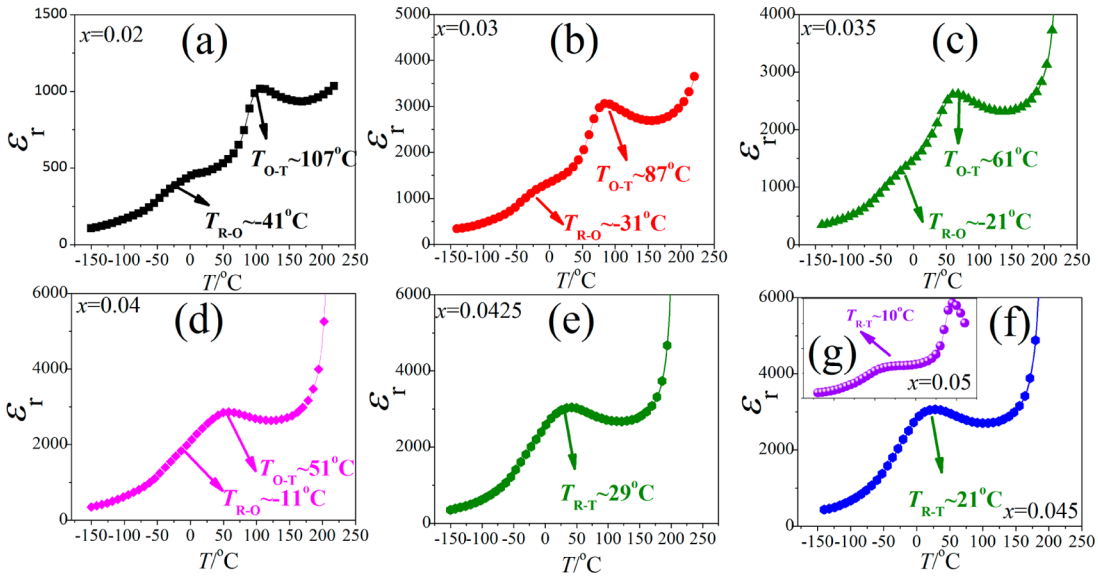

Figure 2. ε_r vs. T curves of the ceramics with (a) x = 0.02, (b) x = 0.03, (c) x = 0.035, (d) x = 0.04, (e) x = 0.0425, (f) x = 0.045, and (g) x = 0.05.

dx.doi.org/10.1021/am500819v | ACS Appl. Mater. Interfaces 2014, 6, 6177−6180

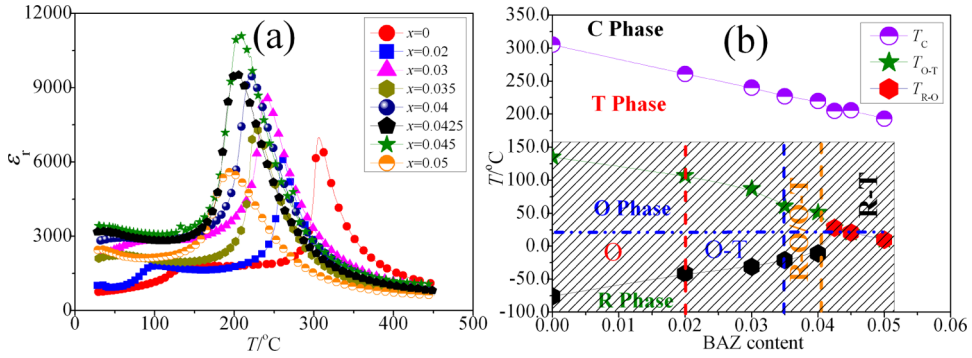

Figure 3. (a) ε_r vs. T curves of the ceramics measured at 30–450 °C, and (b) phase diagram of the ceramics.

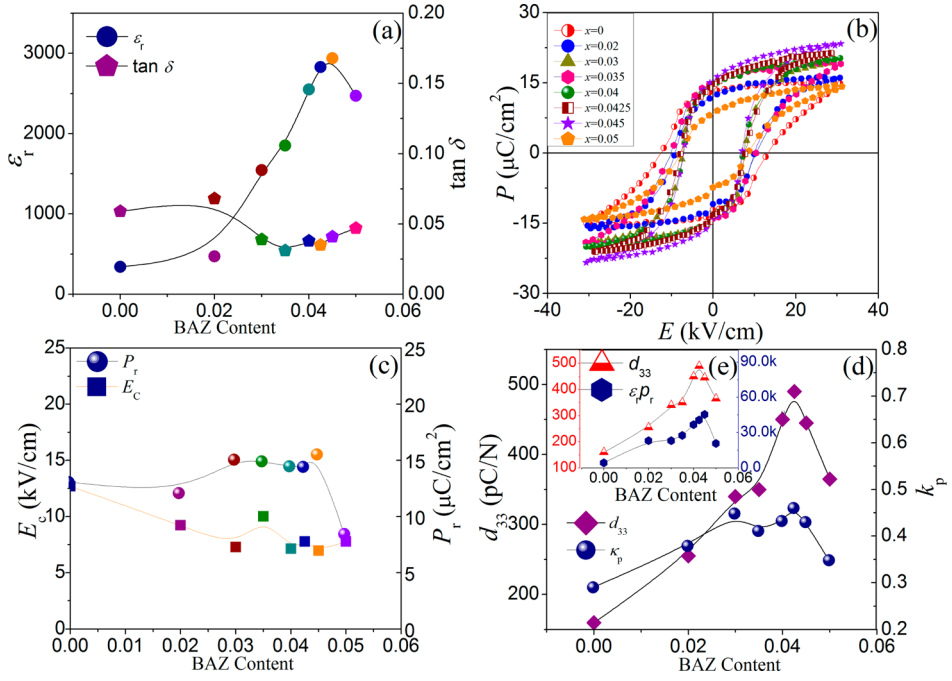

Figure 4. Composition dependence of (a) ε_r and tan δ, (b) P–E loops, (c) P_r and E_C, (d) d_{33} and k_p, and (e) $\varepsilon_r P_r$ and d_{33} vs. BAZ content of the ceramics

process[30–33] and the flattening of a free energy profile is confirmed by Ab initio and phenomenological calculations.[34–37] As a result, the R and T mixed phases are mainly responsible for the giant piezoelectricity. In addition, the d_{33} should also be related to their dielectric and ferroelectric properties, e.g., $d_{33} \approx \alpha \varepsilon_r P_r$.[7] According to this equation, the $\varepsilon_r P_r$ against BAZ content of the ceramic was shown in Figure 4e. A maximum $\varepsilon_r P_r$ was found in the ceramics with R-T phase boundary, which matches the curve of d_{33} vs. BAZ content, showing that their improved $\varepsilon_r P_r$ is partly responsible for the giant d_{33}.

We have achieved a giant d_{33} of ~490 pC/N in $(1-x)(K_{0.48}Na_{0.52})(Nb_{0.95}Sb_{0.05})O_3$-$xBi_{0.5}Ag_{0.5}ZrO_3$ ceramics by designing the R-T phase boundary. The R-T phase boundary was identified in the ceramics with $0.04 < x \leq 0.05$. The ceramic with $x = 0.0425$ possesses a peak d_{33} of ~490 pC/N, showing such a material system can intrigue the researchers in the field of lead-free piezoceramics.

■ ASSOCIATED CONTENT

Supporting Information

Experimental section and FE-SEM images. This material is available free of charge via the Internet at http://pubs.acs.org.

■ AUTHOR INFORMATION

Corresponding Author

*E-mail: msewujg@scu.edu.cn or wujiagang0208@163.com.

Notes

The authors declare no competing financial interest.

■ ACKNOWLEDGMENTS

The authors gratefully acknowledge the supports of the Fundamental Research Funds for the Central Universities (2012SCU04A01), the introduction of talent start funds of Sichuan University (2082204144033), and the National Science Foundation of China (NSFC 51102173, 51272164, 51332003). Thank Ms. Hui Wang for measuring the FE-SEM patterns.

REFERENCES

(1) Saito, Y.; Takao, H.; Tani, T.; Nonoyama, T.; Takatori, K.; Homma, T.; Nagaya, T.; Nakamura, M. Lead-free Piezoceramics. *Nature* **2004**, *432*, 84−87.

(2) Cross, E. Materials science: Lead-free at last. *Nature* **2004**, *432*, 24−25.

(3) Guo, Y.; Kakimoto, K.; Ohsato, H. Phase Transitional Behavior and Piezolectric Properties of $(Na_{0.5}K_{0.5})NbO_3$-$LiNbO_3$ Ceramics. *Appl. Phys. Lett.* **2004**, *85*, 4121−4123.

(4) Hollenstein, E.; Davis, M.; Damjanovic, D.; Setter, N. Piezoelectric Properties of Li-and Ta-modified $(K_{0.5}Na_{0.5})NbO_3$ Ceramics. *Appl. Phys. Lett.* **2005**, *87*, 182905.

(5) Malic, B.; Bernard, J.; Holc, J.; Jenko, D.; Kosec, M. Alkaline-earth Doping in (K,Na)NbO_3 Based Piezoceramics. *J. Eur. Ceram. Soc.* **2005**, *25*, 2707−2711.

(6) Takenaka, T.; Nagata, H. J. Current Status and Prospect of Lead-free Piezoelectric Ceramics. *J. Eur. Ceram. Soc.* **2005**, *25*, 2693−700.

(7) Shrout, T. R.; Zhang, S. Lead-free Piezoceramics: Alternatives for PZT? *J. Electroceram* **2007**, *19*, 111−124.

(8) Lin, D.; Kwok, K. W.; Lam, K. H.; Chan, H. L. Structure and Electrical Properties of $K_{0.5}Na_{0.5}NbO_3$-$LiSbO_3$ Lead-free Piezoelectric Ceramics. *J. Appl. Phys.* **2007**, *101*, 074111.

(9) Wu, J. G.; Xiao, D. Q.; Wang, Y. Y.; Zhu, J. G.; Wu, L.; Jiang, Y. H. Effects of K/Na Ratio on the Phase Structure and Electrical Properties of $(K_xNa_{0.96-x}Li_{0.04})(Nb_{0.91}Ta_{0.05}Sb_{0.04})O_3$ Lead-free Ceramics. *Appl. Phys. Lett.* **2007**, *91*, 252907.

(10) Akdoğan, E. K.; Kerman, K.; Abazari, M.; Safari, A. Origin of High Piezoelectric Activity in Ferroelectric $(K_{0.44}Na_{0.52}Li_{0.04})$-$(Nb_{0.84}Ta_{0.1}Sb_{0.06})O_3$ Ceramics. *Appl. Phys. Lett.* **2008**, *92*, 112908.

(11) Rödel, J.; Kounga, A. B. N.; Weissenberger-Eibl, M.; Koch, D.; Bierwisch, A.; Rossner, W.; Hoffmann, M. J.; Danzer, R.; Schneider, G. Development of A Roadmap for Avanced Ceramics:2010-2025. *J. Eur. Ceram. Soc.* **2009**, *29*, 1549−1560.

(12) Rödel, J.; Jo, W.; Seifert, K.; Anton, E. M.; Granzow, T.; Damjanovic, D. Perspective on the Development of Lead-free Piezoceramics. *J. Am. Ceram. Soc.* **2009**, *89*, 1153−1177.

(13) Damjanovic, D.; Klein, N.; Li, J.; Porokhonskyy, V. What Can. Be Expected from Lead-free Piezoelectric Materials? *Funct. Mater. Lett.* **2010**, *3*, 5−13.

(14) Matsubara, M.; Yamaguchi, T.; Kikuta, K.; Hirano, S. Effect of Li Substitution on the Piezoelectric Properties of Potassium Sodium Niobate Ceramics. *Jpn. J. Appl. Phys., Part 1* **2005**, *44*, 6136−6142.

(15) Park, H. Y.; Cho, K. H.; Paik, D. S.; Nahm, S.; Lee, H. G.; Kim, D. H. Microstructure and Piezoelectric Properties of Lead-free $(1-x)(Na_{0.5}K_{0.5})NbO_3$-$xCaTiO_3$ Ceramics. *J. Appl. Phys.* **2007**, *102*, 124101.

(16) Cheng, X.; Wu, J.; Wang, X.; Zhang, B.; Zhu, J.; Xiao, D.; Wang, X.; Lou, X. Giant d_{33} in (K, Na)(Nb, Sb)O_3-(Bi, Na, K, Li)ZrO_3 Based Lead-free Piezoelectrics with High T_C. *Appl. Phys. Lett.* **2013**, *103*, 052906.

(17) Zang, G. Z.; Wang, J. F.; Chen, H. C.; Su, W. B.; Wang, C. M.; Qi, P.; Ming, B. Q.; Du, J.; Zheng, L. M.; Zhang, S.; Shrout, T. R. Perovskite $(Na_{0.5}K_{0.5})_{1-x}(LiSb)_xNb_xO_3$ Lead-free Piezoceramics. *Appl. Phys. Lett.* **2006**, *88*, 212908.

(18) Chang, Y. F.; Yang, Z.; Ma, D.; Liu, Z.; Wang, Z. Phase Transitional Behavior, Microstructure, and Electric Properties in Ta-modified $[(K_{0.458}Na_{0.542})_{0.96}Li_{0.04}]NbO_3$ Lead-free Piezoelectric Ceramics. *J. Appl. Phys.* **2008**, *104*, 024109.

(19) Gao, Y.; Zhang, J.; Qing, Y.; Tan, Y.; Zhang, Z.; Hao, X. Remarkably Strong Piezoelectric of Lead-free $(K_{0.5}Na_{0.5})_{0.98}Li_{0.02}(Nb_{0.77}Ta_{0.18}Sb_{0.05})O_3$ Ceramics. *J. Am. Ceram. Soc.* **2011**, *94*, 2968−2973.

(20) Zuo, R.; Fu, J. Rhombohedral-Tetragonal Phaes Coexistence and Piezoelectric Properties of (NaK)(NbSb)O_3-$LiTaO_3$-$BaZrO_3$ Lead-free Ceramics. *J. Am. Ceram. Soc.* **2011**, *94*, 1467−1470.

(21) Liang, W. F.; Wu, W. J.; Xiao, D. Q.; Zhu, J. G.; Wu, J. G. Construction of New Morphotropic Phase Boundary in 0.94-$(K_{0.4-x}Na_{0.6}Ba_xNb_{1-x}Zr_x)O_3-0.06LiSbO_3$ Lead-free Piezoelectric Ceramics. *J. Mater. Sci.* **2011**, *46*, 6871−6876.

(22) Zhang, B.; Wu, J.; Cheng, X.; Wang, X.; Xiao, D.; Zhu, J.; Wang, X.; Lou, X. Lead-free Piezoelectric Based on Potassium-Sodium Niobate with Giant d_{33}. *ACS Appl. Mater. Interfaces* **2012**, *4*, 1182−1185.

(23) Matsubara, M.; Kikuta, K.; Hirano, S. Piezoelectric Properties of $(K_{0.5}Na_{0.5})(Nb_{1-x}Ta_x)O_3$-$K_{5.4}CuTa_{10}O_{29}$ Ceramics. *J. Appl. Phys.* **2005**, *97*, 114105.

(24) Li, J. F.; Wang, K.; Zhu, F. Y.; Cheng, L. Q.; Yao, F. Z. (K,Na)NbO_3-Based Lead-free Piezoceramics: Fundamental Aspects, Processing Technologies, and Remaining Challenges. *J. Am. Ceram. Soc.* **2013**, *96*, 3677−3696.

(25) Jaffe, B.; Cook, W. R.; Jaffe, H. *Piezoelectric Ceramics*; Academic: New York, 1971.

(26) Park, S. E.; Shrout, T. R. Characteristics of Relaxor-Based Piezoelectric Single Crystals for Ultrasonic Transducers. *IEEE Trans. Ultrason. Ferr* **1997**, *44*, 1140−1147.

(27) Zuo, R. Z.; Fu, J.; Lv, D. Y. Antimony Tuned Rhombohedral-Rothorhombic Phase Transition and Enhanced Piezoelectric Properties in Sodium Potassium Niobate. *J. Am. Ceram. Soc.* **2010**, *93*, 2783−2787.

(28) Zhang, B.; Wang, X.; Cheng, X.; Zhu, J.; Xiao, D.; Wu, J. Enhanced d_{33} Value in $(1-x)[(K_{0.50}Na_{0.50})_{0.97}Li_{0.03}Nb_{0.97}Sb_{0.03}O_3]$-$xBaZrO_3$ Lead-free Ceramics with An Orthormbic-Rhombohedral Phase Boundary. *J. Alloys Compd.* **2013**, *581*, 446−451.

(29) Wang, X. P.; Wu, J. G.; Xiao, D. Q.; Zhu, J. G.; Cheng, X. J.; Zheng, T.; Zhang, B. Y.; Lou, X. J.; Wang, X. J. Giant Piezoelectricity in Potassium-Sodium Niobate Lead-free Ceramics. *J. Am. Chem. Soc.* **2014**, *136*, 2905−2910.

(30) Damjanovic, D. A Morphotropic Phase Boundary System Based on Polarization Rotation and Polarization Extension. *Appl. Phys. Lett.* **2010**, *97*, 062906.

(31) Yimnirun, R.; Ngamjarurojana, A.; Wongmaneerung, R.; Wongsaenmai, S.; Ananta, S.; Laosiritaworn, Y. Temperature Scaling of Ferroelectric Hysteresis in Hard Lead Zirconate Titanate Bulk Ceramic. *Appl. Phys.* **2007**, *A89*, 737−741.

(32) Smolenskii, G. A.; Taylor, G. W. *Ferroeletrics and Related Materials*; Gordon and Breach Science Publishers: New York, 1984.

(33) Jaffe, B.; Roth, R. S.; Marzullo, S. Piezoelectric Properties of Lead Zirconate-Lead Titanate Solid-Solution Ceramics. *J. Appl. Phys.* **1954**, *25*, 809−810.

(34) Fu, H.; Cohen, R. E. Polarization Rotation Mechanism for Ultrahigh Electromechanical Response in Single-Crystal Piezoelectrics. *Nature* **2000**, *403*, 281−283.

(35) Wu, Z. G.; Cohen, R. E. Pressure-induced Anomalous Phase Transitions and Colossal Enhancement of Piezoelectricity in $PbTiO_3$. *Phys. Rev. Lett.* **2005**, *95*, 037601.

(36) Budimir, M.; Damjanovic, D.; Setter, N. Piezoelectric Response and Free Energy Instability in the Perovskite Crystals $BaTiO_3$, $PbTiO_3$ and $Pb(Zr,Ti)O_3$. *Phys. Rev.* **2006**, *B73*, 174106.

(37) Damjanovic, D. Contributions to The Piezoelectric Effect in Ferroelectric Single Crystals and Ceramics. *J. Am. Ceram. Soc.* **2005**, *88*, 2663−2676.